ADVANCES IN ATMOSPHERIC SCIENCES, VOL. 34, FEBRUARY 2017, 169–180

• **Original Paper** •

Establishment of the South Asian High over the Indo-China Peninsula During Late Spring to Summer

Lijuan WANG*[1], Aiguo DAI[2,3], Shuaihong GUO[4], and Jing GE[1]

[1]*Key Laboratory of Meteorological Disaster, Ministry of Education/Joint International Research Laboratory of Climate and Environment Change/Collaborative Innovation Center on Forecast and Evaluation of Meteorological Disasters/Science and Technology Innovation Team on Climate Simulation and Forecast, Nanjing University of Information Science and Technology, Nanjing* 210044*, China*

[2]*Department of Atmospheric and Environmental Sciences, University at Albany, SUNY, Albany, NY* 12222*, USA*

[3]*National Center for Atmospheric Research, Boulder, Colorado* 80307*, USA*

[4]*Meteorological Observatory of No.* 95147 *Unit of PLA, Meizhou* 514593*, China*

(Received 4 April 2016; revised 20 July 2016; accepted 25 August 2016)

ABSTRACT

The establishment of the upper-level South Asian high (SAH) over the Indo-China Peninsula (ICP) during late boreal spring and its possible causes are investigated using long-term NCEP–NCAR and ERA-40 reanalysis and satellite-observed OLR data. Results show that, from early March to mid-April, deep convection stays south of ~6°N over the northern Sumatran islands. As the maximum solar radiation moves over the latitudes of the ICP (10°–20°N) in late April, the air over the ICP becomes unstable. It ascends over the ICP and descends over the adjacent waters to the east and west. This triggers deep convection over the ICP that induces large latent heating and strong updrafts and upper-level divergence, leading to the formation of an upper-level anticyclonic circulation and the SAH over the ICP. During early to mid-May, deep convection over the ICP intensifies and extends northwards to the adjacent waters. Strong latent heating from deep convection enhances and maintains the strong updrafts and upper-level divergence, and the SAH is fully established by mid-May. Thus, the seasonal maximum solar heating and the land–sea contrast around the ICP provide the basic conditions for deep convection to occur preferentially over the ICP, which leads to the formation of the SAH over the ICP from late April to mid-May. Simulations using RegCM4 also indicate that the diabatic heating over the ICP is conducive to the generation and development of upper-level anticyclonic circulation, which leads to an earlier establishment of the SAH.

Key words: South Asian high, Indo-China Peninsula, diabatic heating, deep convection

Citation: Wang, L. J., A. Dai, S. H. Guo, and J. Ge, 2017: Establishment of the South Asian high over the Indo-China Peninsula during late spring to summer. *Adv. Atmos. Sci.*, **34**(2), 169–180, doi: 10.1007/s00376-016-6061-7.

1. Introduction

The South Asian high (SAH) is the strongest high-pressure system in the upper troposphere in boreal summer over the Asia–Pacific region. It covers a large area from South Asia to the western Pacific. The SAH is a major component of the Asian summer monsoon system and acts as a linkage between the tropical and Asian monsoon circulations (Flohn, 1960; Mason and Anderson, 1963; Tao and Zhu, 1964; Rodwell and Hoskins, 2001; Miyasaka and Nakamura, 2005; Tang and Guan, 2015). The SAH is also referred to as the Tibetan high, as it moves to, and often stays over, the Tibetan Plateau during boreal summer.

Before its seasonal movement towards the Tibetan Plateau in early June, the position and strength of the upper lever anticyclone vary considerably during the preceding months of boreal winter and spring. The center of the upper-level anticyclone is usually located east of the Philippines over the western Pacific before March, moves westward in April, and the SAH finally establishes over the Indo-China Peninsula (ICP) during late April and early May. In late May, the SAH starts to move towards the Tibetan Plateau, and arrives there typically around 7 June (Luo et al., 1982; Zhu et al., 1980; He et al., 2003). Luo et al. (1982) noted that there are four distinct northward jumps of the SAH ridge line at 120°E, with the first jump around 16 May; the second crossing 25°N from 5 to 10 June, which marks the onset of meiyu monsoon rainfall over the middle to lower reaches of the Yangtze valley; the third occurring around late June to early July, with the SAH ridge traveling from 28°N to 31°N; and the final jump happening around 10–15 July, with the ridge line reaching 33°N.

Qian et al. (2002) divided the SAH seasonal cycle into

* Corresponding author: Lijuan WANG
Email: wljfw@163.com

two states: a winter and a summer mode. In winter (October–April), the upper-level anticyclone is located over the western Pacific Ocean (140°–170°E), with its ridge line south of 15°N. The winter upper-level anticyclone is relatively weak and covers a small area. In summer (May–September), the SAH is over the Asian continent, with its ridge line around 30°N, one of its two centers positioned over the Tibetan Plateau (90°E), and the other over the Iranian Tableland (60°E). There is, however, a different view (Liu et al., 2000) that considers the high over Pacific waters in winter and the summer SAH as independent systems, with the former being dynamic and the latter being thermal-driven. Thus, the transition period from winter to summer, especially from late spring to early summer, is very important for investigating upper-level anticyclone activities.

As a vigorous upper-level circulation system, the south–north swing of the SAH's ridge line, the east–west oscillation of its center, and its seasonal northward jump and southward withdrawal, greatly impact the onset and movement of the whole East Asian summer monsoon and the advance and maintenance of the monsoon rainbelt over East China (Zhu and He, 1985; Wu and Zhang, 1998; Li and Mu, 2001; Zhang and Qian, 2002; Tan et al., 2005; Yang and Li, 2005; Zhang et al., 2006; Ke and Guan, 2014; Han et al., 2015; Lu et al., 2015). The activities of the upper-level anticyclone from late spring to early summer are associated with the establishment of the summer monsoon over the South China Sea (SCS) (Qian et al., 2004). Because of weak influences from the surface, the seasonal movements of the anticyclone at upper levels are more distinguishable and earlier than the changes of wind at lower levels (Liu et al., 2004; Qian et al., 2004). Qian et al. (2004) suggested that the swift westward movement of the upper-level anticyclone from the western Pacific Ocean into the ICP around the end of April is a precursor to the imminent seasonal transition, meaning the location of the SAH can be used to predict the onset time of the Asian tropical summer monsoon.

Figure 1 shows the long-term mean streamline and geopotential height fields at the 150-hPa level for 14 April, 26 April and 10 May, based on NCEP–NCAR (left-hand column) and ERA-40 (right-hand column) reanalysis data. The two reanalyses exhibit broadly consistent features, with only some small-scale differences. Around mid-April, the upper-level anticyclone is over the waters southeast of the Philippines (Figs. 1a and d). Subsequently, the anticyclone moves westward and, around late April, it evolves into a two-cored structure, with one core situated over the waters southeast of the Philippines and the other over the southeastern part of the ICP (Figs. 1b and e). Such a two-cored structure is maintained until early May, when the western core intensifies and moves northwestward to the ICP and the anticyclone's ridge line moves from 10°N to around 15°N, accompanied by a 14285-gpm center in the height field (Figs. 1c and f). This marks the initial establishment of the SAH over the ICP. By mid- to late May, the western circulation center stays steadily over the ICP and intensifies further, in contrast to the eastern core which continues to weaken to divergent flow (not shown). At that time, the SAH is fully established over the ICP. According to Liu et al. (2013), the convection over the southern Philippines can excite the initial appearance of the SAH over the southern SCS around 20 April. Why, then, does the SAH travel westward rapidly from the SCS to the ICP around the end of April? What are the causes of this westward movement? Is it related to the thermal heating over the ICP? Does this movement resemble the SAH's migration towards the Tibetan Plateau, which follows the seasonal maximum thermal heating over Asia (Qian et al., 2002; Liu et al., 2004)? These questions will be discussed in this study.

2. Data and method

We use NCEP–NCAR (Kalnay et al., 1996) and ERA-40 (Uppala et al., 2005) reanalysis daily data on a $2.5° \times 2.5°$ grid for atmospheric winds, temperature, specific humidity, geopotential height, and surface fields. Satellite-observed daily data of OLR for 1979–2008 from NOAA are also used to show areas with deep convection.

The atmospheric total diabatic heating rate (Q_1) is estimated using the apparent heat sources computed with the inverse calculation scheme developed by Yanai et al. (1973), which takes the form of

$$Q_1 = C_p \left[\frac{\partial \overline{T}}{\partial t} + \overline{\boldsymbol{V}} \cdot \nabla_p \overline{T} + \left(\frac{p}{p_0} \right)^{\frac{R}{C_p}} \overline{\omega} \frac{\partial \overline{\theta}}{\partial p} \right], \qquad (1)$$

where C_p is the specific heat of air, T is air temperature, p_0=1000 hPa, p pressure, θ potential temperature, $\boldsymbol{V}$ horizontal vector winds, ω vertical pressure velocity, and R is the gas constant of air. An overbar indicates it is a grid-box mean. Integrating over the whole air column, we have

$$\langle Q_1 \rangle = \frac{1}{g} \int_{p_t}^{p_s} Q_1 dp \approx LP + S + \langle Q_R \rangle , \qquad (2)$$

where $\langle\ \rangle$ is integrating over the whole air column, p_s is the surface pressure and p_t is the upper limit (set to 100 hPa), L is the latent heat of condensation, P is precipitation, LP is the latent heat flux, S is the surface sensible heat flux, $\langle Q_R \rangle$ is the vertically integrated radiative heating rate, and g is the gravitational constant of Earth.

The model used in this study is RegCM4, based on RegCM3 (Giorgi et al., 2012). In recent years, many researchers have used RegCM4 to simulate the climate mean, extreme climate events and precipitation anomalies in the East Asian monsoon region and found it to perform well in simulating the East Asian climate (Zou and Xie, 2012; Gong et al., 2015; Zhang et al., 2015).

The simulation domain in this study covers central and southern China, the Indian Ocean, the SCS, and western Pacific regions, with the center located at (15°N, 120°E). The horizontal resolution is 100 km (120×80 grid points) and there are 18 vertical levels. A Lambert projection is performed and the integration time step is 180 s. Physical packages include the Grell cumulus parameterization scheme with

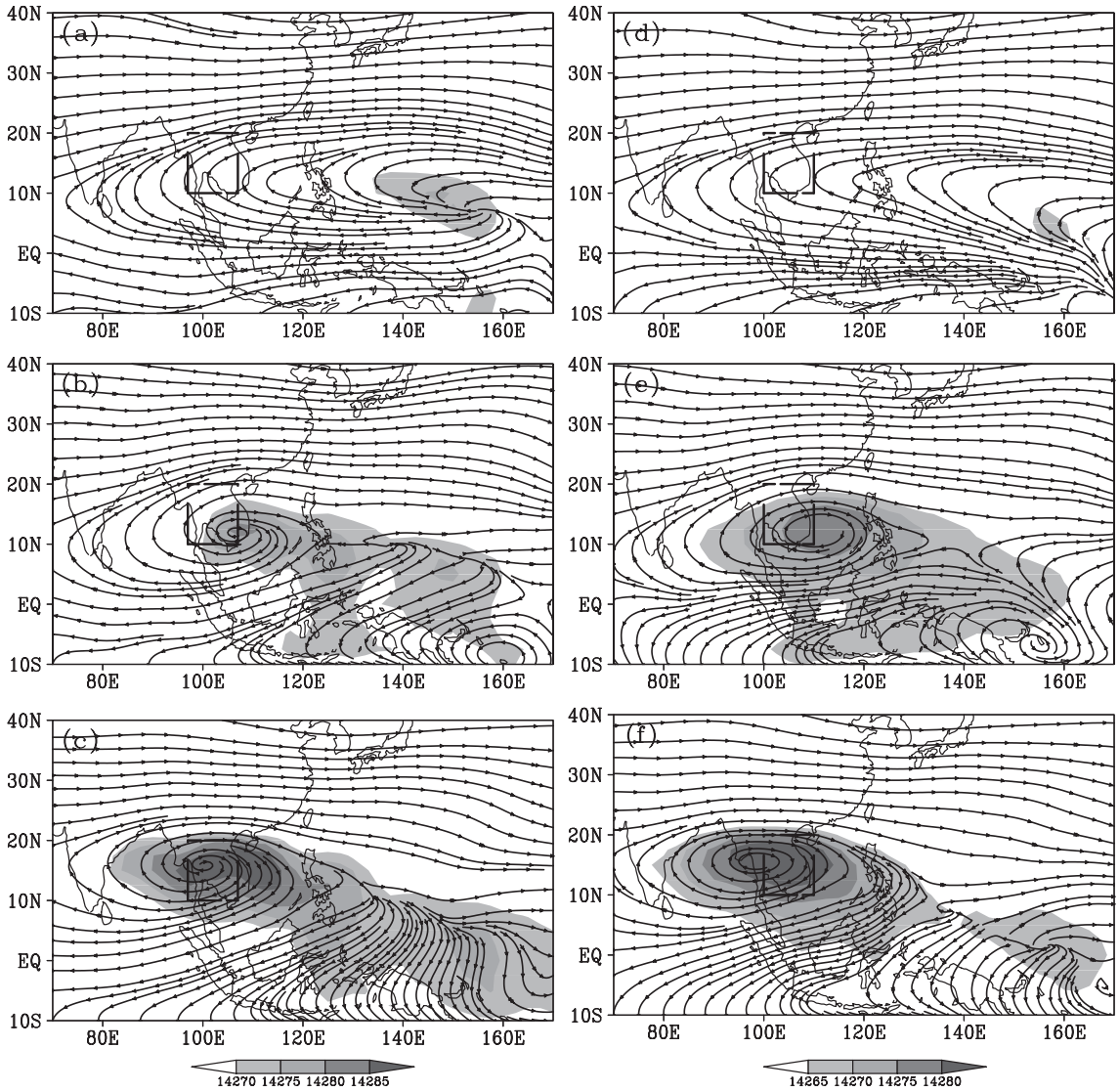

Fig. 1. Long-term mean streamline and geopotential height (shading; units: gpm) fields at 150 hPa from the (a–c) NCEP–NCAR (1979–2008 mean) and (d–f) ERA-40 (1979–2001 mean) reanalysis data for (a, d) 14 April, (b, e) 26 April, and (c, f) 10 May. Dotted box areas represent ICP (10°–20°N，97°–107°E).

the closure assumptions of Fritsch and Chappell, the PBL scheme of Holtslag et al. (1990), the lateral boundary scheme of exponential relaxation approximation, and the ocean flux parameterization scheme of Zeng et al. (1998).

3. Establishment of the SAH over the ICP and associated convection

3.1. *Evolution of OLR around the ICP from March to June*

Low values (<240 W m^{-2}) of OLR from satellite observations are often associated with cold high-cloud tops formed during deep convection, and thus are used to locate deep convection at low latitudes (Haque and Lal, 1991). Figure 2 shows the time–longitude (top) and time–latitude (bottom) cross section of the 1979–2008 mean OLR averaged over the ICP region. The OLR data (Fig. 2a) suggest that deep convection appears first over the ICP (97°–107°E) around 24–25 April, and then extends west- and eastward into the eastern part of the Bay of Bengal (BOB, 85°–97°E) in early May and into the SCS (110°–120°E) in mid-May when the summer monsoon begins. Further examination reveals that the onset of deep convection over the ICP coincides with the time when the upper-level anticyclone splits into a two-cored structure (cf. Figs. 1b and e).

Figure 2b suggests that deep convection in the ICP sector (97°–107°E) stays over Sumatra, south of 6°N, in March, slowly moves northward in early–mid April, and then jumps northward abruptly in late April to cover the whole ICP (10°–20°N). He et al. (2006) also drew the same conclusion. In May and June, deep convection over the ICP becomes stronger when the SAH core sits steadily over the ICP. The sudden northward jump of the deep convection zone from

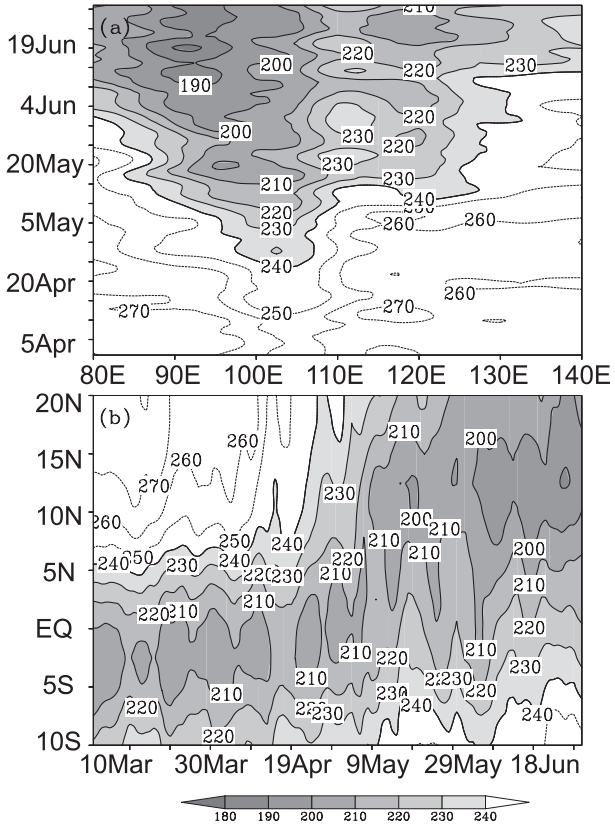

Fig. 2. The (a) longitude–time (averaged over 10°–20°N) and (b) latitude–time (averaged over 97°–107°E) cross section of satellite-observed 1979–2008 mean OLR (units: W m^{-2}). Shaded areas represent active convection. The solid (dashed) lines denote OLR values less (greater) than 240 W m^{-2}.

Sumatra to the ICP around late April coincides with the establishment of the upper-air SAH over the ICP.

It is well known that latent heat released during deep convection can influence the atmospheric thermal state, thereby affecting atmospheric circulation (Liu et al., 1999, 2004; Wu et al., 2015). What, therefore, are the characteristics of the atmospheric heating over the ICP before, during and after active convection from April to June? What are the changes in the associated atmospheric circulation? Do the changes of atmospheric heating in this period play a key role in the SAH's establishment over the ICP? To address these questions, we next analyze the atmospheric diabatic heating rate (Q_1) and meridional circulation over the ICP during this period.

3.2. *Evolution of diabatic heating, vertical velocity and meridional circulation from April to June*

Based on the daily evolution of 150-hPa streamline and height fields, we focus on three key phases for the SAH's establishment over the ICP: the pre-establishment (11–20 April), initial establishment (24 April to 3 May), and late stage of establishment (6–15 May). Figure 3 shows the latitude–height cross section of the 1979–2008 mean atmospheric diabatic heating rate (Q_1, contours), vertical velocity (shading), and meridional-vertical circulation (arrows) averaged over 97°–107°E for the three aforementioned phases of the establishment of the SAH. During the pre-establishment phase, the diabatic heating center in the mid–upper troposphere (500–400 hPa) is located mainly over northern Sumatra (0°–6°N), where strong rising motion also occurs (Fig. 3a). Combined with the OLR data (Fig. 2), these results suggest that convection is very active over northern Sumatra during the pre-establishment phase, leading large latent heating in the mid–upper troposphere there. During this period, the diabatic heating (<2.5 K d^{-1}) over the ICP (10°–20°N) is relatively weak and centered below 600 hPa, which indicates that convection is shallow and is not fully developed at this time (Fig. 3a).

During the initial establishment phase (24 April to 3 May) of the SAH, the diabatic heating (up to 3.5 K d^{-1}) and vertical motion over the ICP become stronger and deeper, with vigorous updrafts reaching 200 hPa and over a larger domain (Fig. 3b). Vigorous deep convection over the ICP releases large amounts of latent heat and causes strong upper-level divergence to facilitate the formation of an anticyclone at higher levels over this region. This leads to the formation of the strong core of the SAH over the ICP during late April to early May, which is in agreement with Fig. 1b. At the same time, the diabatic heating and vertical motion over northern Sumatra weaken and spread northward towards the ICP, which help enhance the rising motion over the ICP (Fig. 3b).

During the late stage (6–15 May) of the SAH's establishment (Fig. 3c), the diabatic heating and vertical motion over the ICP become even more vigorous, while they are very weak and diffused over northern Sumatra. Figures 2b and 3c together suggest that the center of deep convection is now located over the ICP. The convection releases still more latent heat, leading to a heating rate of 2.5 K d^{-1} and enhanced divergence at the 150-hPa level.

The above results show that the northward movement of the deep convection center from northern Sumatra to the ICP from mid-April to early May plays a key role in the establishment of the SAH over the ICP during this same period. From late April to early May, the deep convection moves rapidly from northern Sumatra into the southern ICP. This leads to strong diabatic heating in the mid–upper troposphere and causes large divergence at the 150-hPa level, thereby forming an anticyclone (i.e., the SAH) over the ICP during late April to early May. By mid-May, convection is also very active and deep over the BOB and the SCS (Fig. 2a). The tropospheric latent heating and upper-level divergence produced by these convective activities around the ICP further enhance the upper-level anticyclone over the region. This marks the full establishment of the SAH over the ICP.

4. Causes of the northward jump of convection

The remaining question is why the center of deep convection jumps to the ICP from northern Sumatra during late April to early May. Naturally, one may relate this to the seasonal

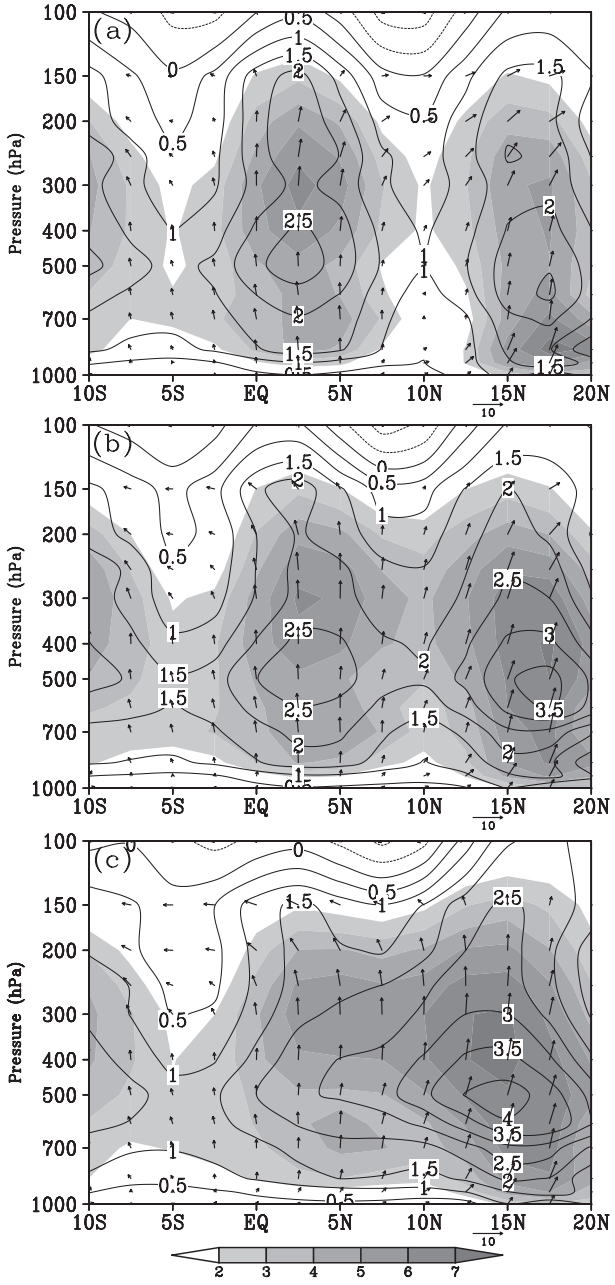

Fig. 3. Latitude–height cross sections of the 1979–2008 mean atmospheric diabatic heating rate (Q_1; contours; units: K d^{-1}), vertical velocity ($-\omega\times10^{-2}$; shading; units: Pa s^{-1}), and meridional and vertical winds (vectors; units: m s^{-1}), averaged over 97°–107°E, for (a) 11–20 April, (b) 24 April to 3 May, and (c) 6 May to 15 May, based on NCEP–NCAR reanalysis data.

movement of the maximum solar heating. Figure 4 shows the latitude–time cross section of the 1979–2008 mean clear-sky downward solar radiation at the surface averaged over the ICP sector (97°–107°E). It can be seen that the maximum solar heating moves northward from around 5°S on 5 March to around 15°N in late April to early May. It is clear that the abrupt northward jump of deep convection from northern Sumatra to the ICP during late April (Fig. 2b) coincides with the significant enhancement of the maximum solar heating in late April over the ICP (Fig. 4). In particular, the contour lines of 355 W m^{-2}, or larger jumps from south of the Equator in early March to the ICP (10°–20°N) in late April, indicate the onset of strong seasonal solar heating over the ICP.

Figure 5a shows that solar radiation over the ICP increases rapidly from early March to late April, when it peaks. With the large solar heating over the ICP land areas, the geopotential height difference at 150 hPa between the ICP and the waters east of the Philippines also increases during this period, and it reverses sign (i.e., with larger height over the ICP than over the sea) in late April (Fig. 5a). This marks the initial stage of the SAH's establishment.

The change in the sensible heat flux caused by the increased surface solar radiation flux is much greater over the continent than over the ocean (Fig. 5b). Compared to the BOB and SCS at the same latitude, the sensible heating is stronger over the ICP, which can arouse ascending motion along the lateral boundary of the ICP, and converge the air from the surrounding areas in the lower layer to the upper troposphere. When water vapor is sufficient, this effect can enhance the potential instability of the atmosphere and trigger convection.

Figures 5a and c suggest that the increase in the geopotential height over the ICP is closely associated with the increased atmospheric diabatic (mostly latent) heating over the ICP, and the increases in atmospheric latent heating come from intensifying convection over the ICP during late April and early May (Fig. 2). Thus, atmospheric deep convection and the associated latent heating are together the primary cause for the development of the SAH over the ICP in late April and early May.

Figure 6 further illustrates the differences in diabatic heating, divergence and vertical motion between the ICP and the waters to the east and west at the same latitudes. During all three phases of the SAH's establishment from mid-April to mid-May, air rises over the ICP sector (97°–107°E). From 11 to 20 April (Fig. 6a), the ascending motion over the ICP

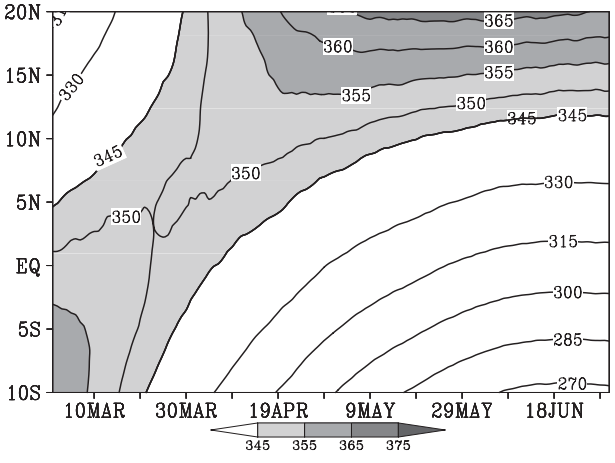

Fig. 4. Latitude–time cross section of 1979–2008 mean clear-sky downward solar radiation (units: W m^{-2}) averaged over 97°–107°E, based on NCEP–NCAR reanalysis data.

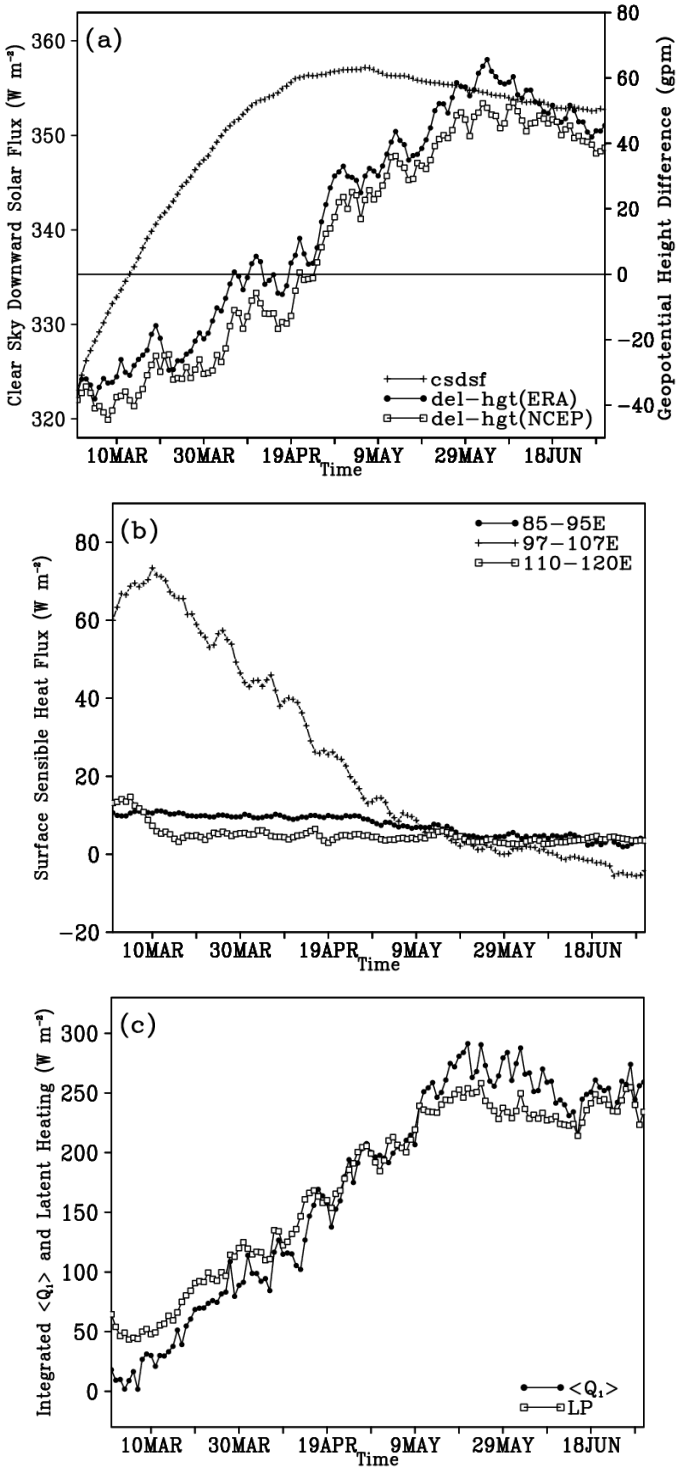

Fig. 5. (a) Seasonal evolution of 1979–2008 mean clear-sky downward solar radiation (plus signs; units: W m^{-2}) averaged over the ICP (10°–20°N, 97°–107°E), and the geopotential height difference (units: gpm) at 150 hPa between (10°–20°N, 97°–107°E) and (10°–20°N, 140°–150°E), based on NCEP–NCAR (open rectangles) and ERA-40 (black dots) reanalysis data. (b) Seasonal evolution of 1979–2008 mean surface sensible heat flux (units: W m^{-2}) averaged over the ICP [(10°–20°N, 97°–107°E); plus signs], BOB [(10°–20°N, 85°–95°E); black dots], and SCS [(10°–20°N, 110°–120°E); open rectangles], based on NCEP–NCAR reanalysis data. (c) Seasonal evolution of the 1979–2008 mean atmospheric integrated total diabatic heating ($\langle Q_1 \rangle$; black dots; units: W m^{-2}) and latent heating (open rectangles; units: W m^{-2}) averaged over the ICP (10°–20°N, 97°–107°E), based on NCEP–NCAR reanalysis data.

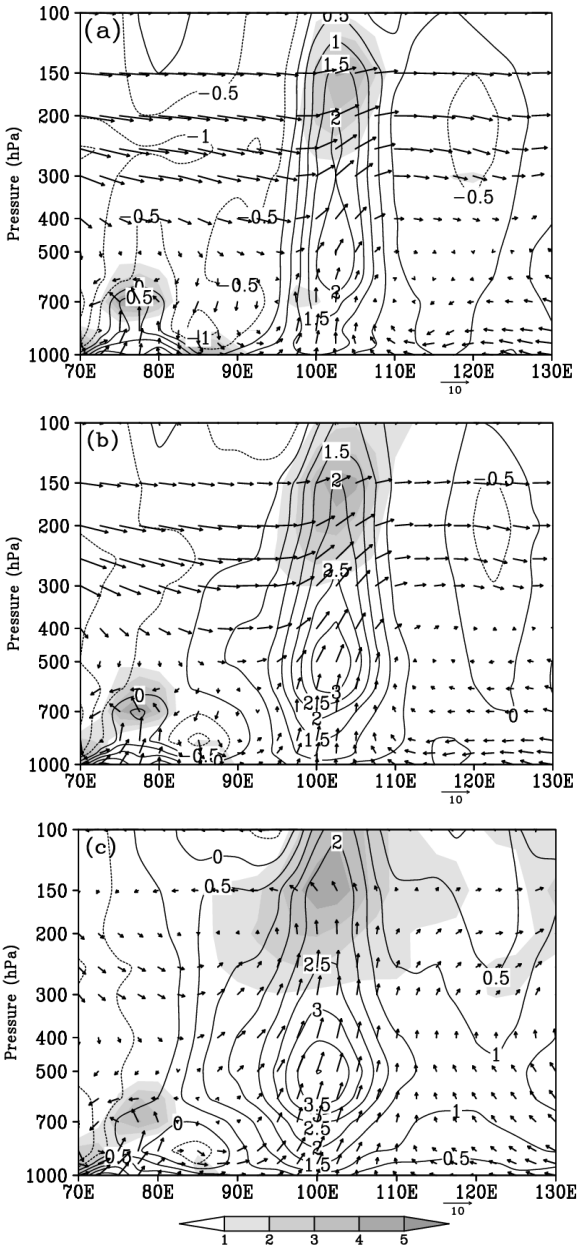

Fig. 6. Longitude–height cross section of the 1979–2008 mean atmospheric diabatic heating rate (contours; units: K d^{-1}), divergence (shading; units: 10^{-6} s^{-1}), and zonal and vertical winds (arrows; units: m s^{-1}) averaged over 10°–20°N for (a) 11–20 April, (b) 24 April to 3 May, and (c) 6–15 May, based on NCEP–NCAR reanalysis data.

appears throughout the entire troposphere, while descending motion appears over the western BOB, which is consistent with the theory of Rodwell and Hoskins (1996) that deep convective heating can excite westward moving Rossby waves that induce subsidence to the west of the diabatic heating. During 24 April to 3 May (Fig. 6b), the ascending motion over the ICP enhances and weak air rises over the eastern BOB, which favors the onset of the BOB summer monsoon (Liu et al., 2013). During 6–15 May (Fig. 6c), the ascending motion over the SCS and eastern BOB further enhances, especially over the ICP regions. The intensity of the rising motion and upper-level divergence over the ICP increases from mid-April to mid-May, while the changes over the adjacent waters are relatively small during the same period. These results help explain why deep convection starts first over the ICP in late April, rather than over the waters to the east and west Fig. 2a. They show that, as the maximum solar heating jumps to 10°–20°N in late April (Fig. 4), large surface sensible heat fluxes over the ICP land areas make the air there relatively unstable compared with the air over the waters to the east and west. This leads to rising motion and deep convection over the ICP land areas and mostly descending motion over the adjacent waters in March and April (Fig. 6). Strong latent heating from deep convection (Fig. 5b) maintains and enhances the updrafts and upper-level divergence, causing an anticyclonic high-pressure center (i.e., the SAH) over the ICP from late April to mid-May.

From the above, the establishment of the SAH is closely associated with the thermal heating over the ICP. The movement of the upper-level anticyclone from the western Pacific waters to the ICP following the maximum diabatic heating from late April to mid-May resembles the SAH's migration towards the Tibetan Plateau from late May to early June, which also follows the seasonal maximum thermal heating over Asia (Qian et al., 2002; Liu et al., 2004).

5. Numerical simulations of the establishment of the SAH over the ICP

The above analysis indicates that the establishment of the SAH over the ICP during April to May is closely associated with the onset of convection there. Using RegCM4, the process of the SAH's establishment is simulated in a series of sensitivity experiments in which we change the atmospheric heating over the ICP. The simulations are performed for the year 2004, which was featured a typical establishment of the SAH over the ICP accompanied by a two-cored structure (Hu, 2006). The initial and lateral boundary conditions are from the NCEP–NCAR reanalysis data for that year, with a resolution of $2.5° \times 2.5°$ at 6-h intervals, including air temperature, geopotential height, vertical velocity, relative humidity, meridional and zonal wind, surface pressure, and other physical fields. The weekly mean SST data on a $1° \times 1°$ grid are used to drive RegCM4. The simulations run from 1 April 2004 to 31 May, producing one output per day. The sensitivity experiments are designed as follows (Figs. 7a and b):

(1) Positive heating anomaly experiment (EX+): A diabatic heating anomaly, with a heating rate of 8 K d^{-1} and centered at (15°N, 102°E), is placed over the ICP at 387 hPa. In the horizontal direction, there are nine grids on both the east and west sides of the center and eleven grids on both the north and south sides. The heating rate decreases to zero in the form of a cosine function from the center to the boundary. In the vertical direction, the heating decreases at a certain rate from the center to the upper and lower levels, respectively.

Other conditions are the same as in the control experiments.

(2) Negative heating anomaly experiment (EX−): Apart from the heating anomaly over the ICP being multiplied by −1 both in the horizontal and vertical direction, all other conditions are the same in EX− as in EX+.

In the 200-hPa streamline fields in the control run (Figs. 8a–c), the anticyclonic circulation splits into two centers in the fifth pentad of April, with one lying above the ICP (the west center) and the other above the ocean to the east of the Philippines (the east center), i.e., a "two-cored" structure. Thereafter, the west center continues to develop and enhance, while the east one weakens. The duration of the SAH's

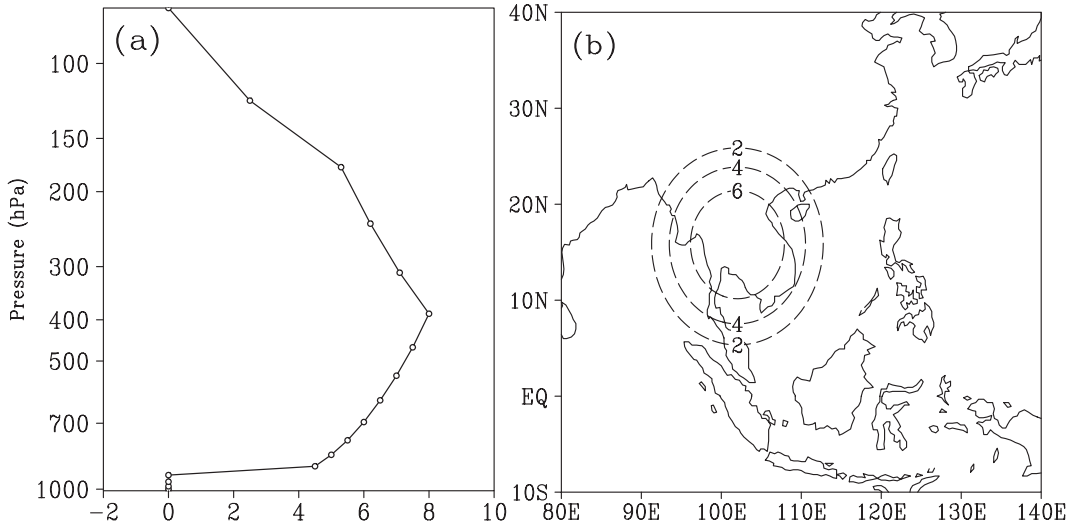

Fig. 7. (a) Vertical profile of the heating rates prescribed in EX+ over the ICP (units: K d^{-1}). (b) Horizontal distribution of the diabatic heating in EX+ (units: K d^{-1}).

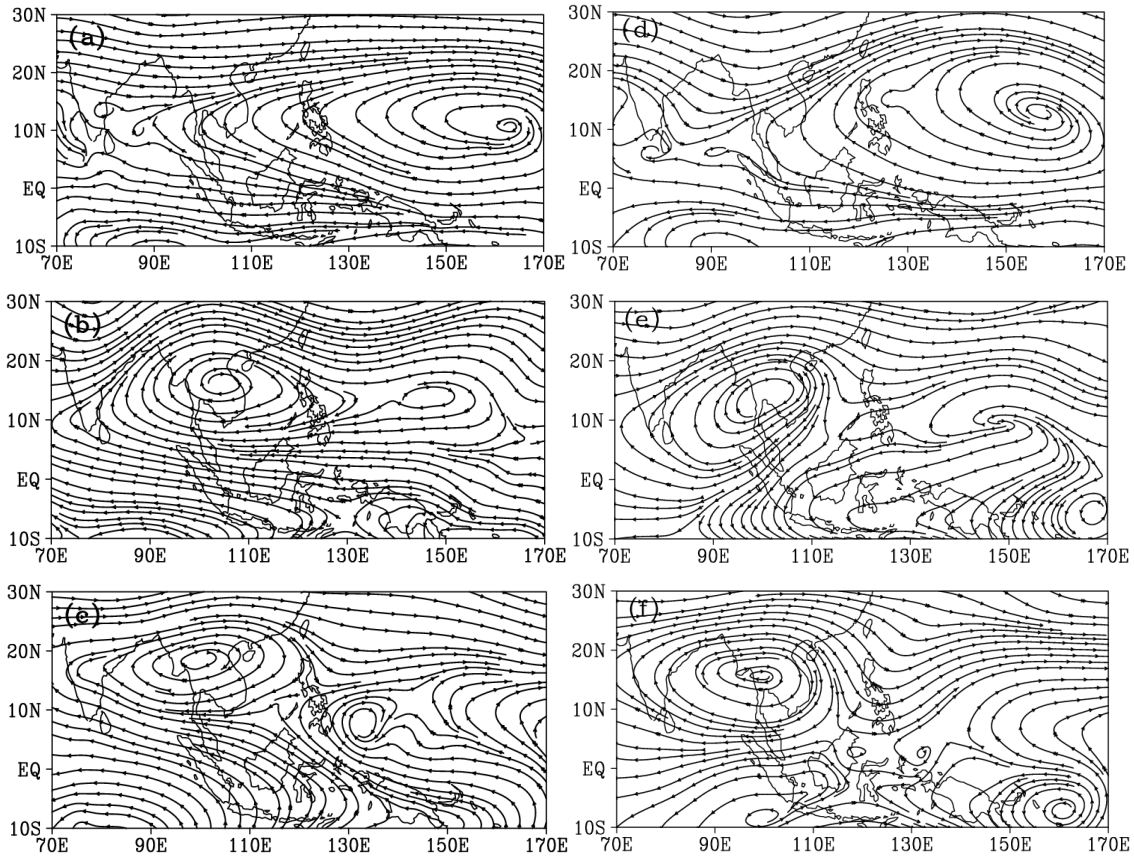

Fig. 8. The streamline fields at 200 hPa in 2004 from the (a–c) control run and (d–f) NCEP–NCAR reanalysis, for the (a, d) third pentad of April, (b, e) fifth pentad of April, and (c, f) first pentad of May.

establishment is from late April to early May. The simulated characteristics of the westward and northward movement of the anticyclonic circulation over South Asia—from the ocean to east of the Philippines, to the ICP through a split of the center—are consistent with the results from the NCEP–NCAR reanalysis data (Figs. 8d–f). Therefore, RegCM4 performs well in simulating the establishment of the SAH.

Figure 9 shows the pentadly evolution of the streamline fields at 200 hPa in the positive heating anomaly experiment over the ICP (EX+) and the difference between EX+ and control runs. The marked discrepancies exist at the beginning of the establishment of the SAH, so the differences from the third pentad to the fifth pentad of April are presented here. The center of anticyclonic circulation over the ocean to the east of the Philippines starts to split up in the fourth pentad of April. A center appears over the eastern BOB and ICP (Fig. 9a), which marks the initial establishment of the SAH over the ICP. Subsequently, the west center keeps developing and strengthening (Figs. 9b and c), and then steadily remains over the ICP in the sixth pentad of April, indicating the full establishment of the SAH. From the difference between EX+ and the control runs, it is apparent that an anticyclonic circulation anomaly appears over the BOB to the western ICP in the third pentad of April, corresponding to the negative vorticity anomaly (Fig. 9d). As the anticyclonic circulation anomaly expands over the whole ICP, the SAH completes its establishment over the region (Figs. 9e and f). Compared to the results from the control run, the start time of the SAH's establishment is one pentad earlier in EX+. Additionally, the time when the SAH is fully established over the ICP is two pentads earlier.

From the pentadly evolution of the streamline fields at 200 hPa in EX− (Fig. 10), it is apparent that the center of anticyclonic circulation is located over the ocean to the east of the Philippines in the third and fourth pentads of April. The ICP region is located on the periphery of the anticyclonic circulation (Fig. 10a). Compared to the results from the control run, the anticyclonic circulation over the ICP is weakened in EX−. Thereafter, the anticyclonic circulation center keeps moving westward to the SCS in the fifth pentad of April, rather than splitting into two centers (Fig. 10b). The center moves to the ICP in the sixth pentad of April (Fig. 10c), which marks the initial establishment of the SAH. From the difference between EX− and the control runs, it is found that the regions including the whole ICP and its northern areas are controlled by the cyclonic circulation anomaly from the third to the fifth pentad of April. The positive vorticity anomaly maintains over the region, which is not conducive

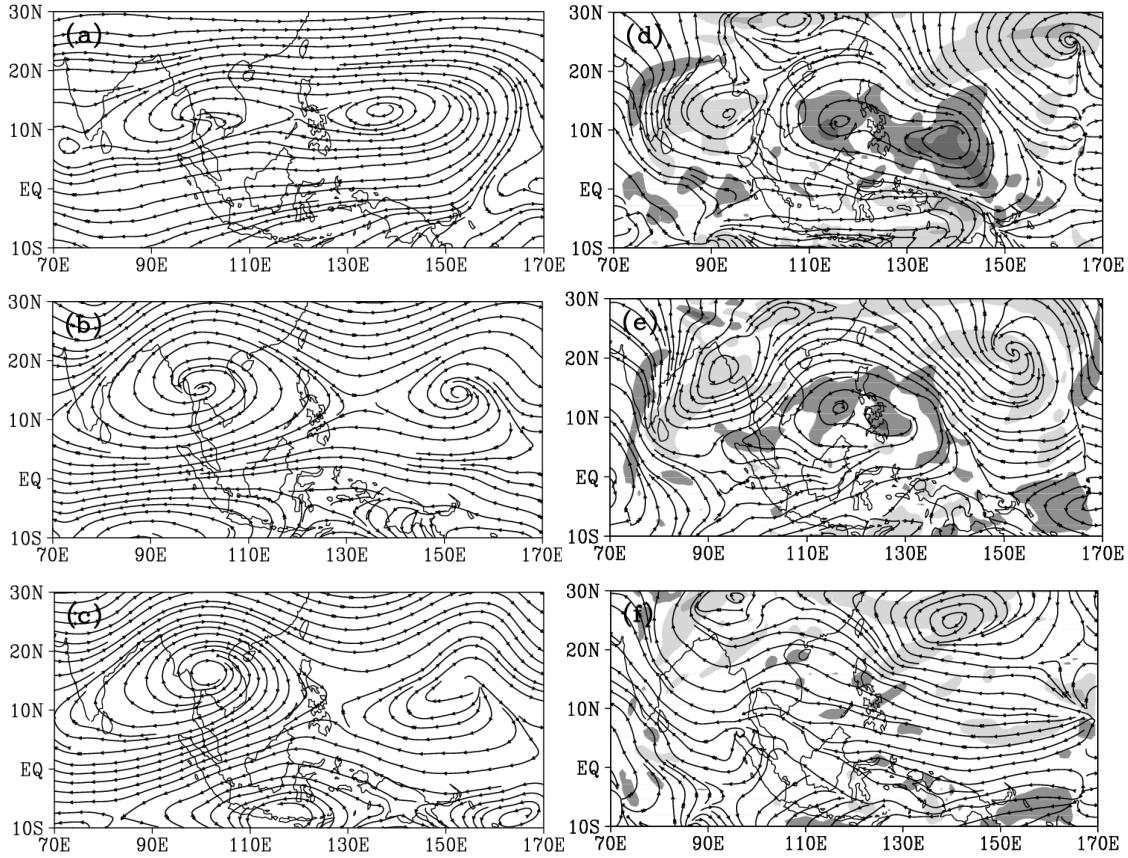

Fig. 9. The streamline fields at 200 hPa in EX+ over the (a–c) ICP for the (a) fourth pentad of April, (b) fifth pentad of April, and (c) sixth pentad of April, and the (d–f) difference in streamline fields and relative vorticity (values greater than 1 are in dark shading and less than −1 in light shading; units: 10^{-5} s^{-1}) between EX+ and the control run for the (d) third pentad of April, (e) fourth pentad of April, and (f) fifth pentad of April.

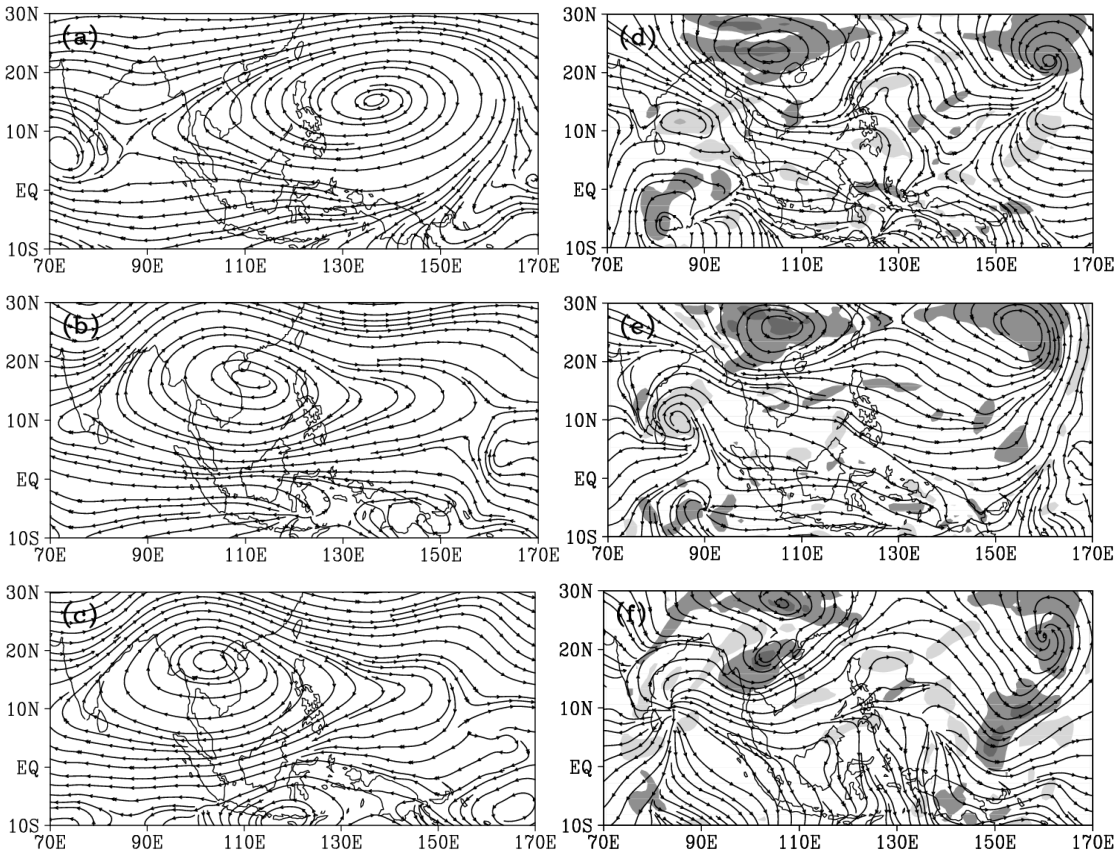

Fig. 10. As in Fig. 9 but for the EX−.

to the establishment of the SAH over the ICP (Figs. 10d–f). It should be noted that there is no split in the anticyclonic circulation center during the process of the SAH's establishment. Thus, the SAH's establishment in EX—is significantly different from that in EX+. The SAH is established in EX− through the gradual westward movement of the anticyclonic circulation center to the ICP, rather than through disintegrating into two centers. In addition, the time when the SAH is fully established over the ICP is one pentad later than the result from the control run. According to the above results, the diabatic heating released from deep convection over the ICP from spring to summer is in favor of the establishment of SAH.

6. Summary

In this study we analyze reanalysis and satellite data to investigate the processes that lead to the formation of the upper-level (150 hPa) SAH over the ICP from late April to mid-May. Both the NCEP–NCAR and ERA-40 reanalysis data show that, from late April to early May, the upper level anticyclone migrates swiftly from western Pacific waters to the ICP, with the upper-level anticyclonic circulation gradually weakening over the waters east of the Philippines. During this period, the 150-hPa circulation over this region shows a "two-cored" structure, with a strong core over the ICP and a weak core over the Pacific Ocean southeast of the Philippines. The strong center over the ICP, referred to as the SAH, stays over the ICP until late May.

Satellite OLR data show that deep convection over the ICP sector (97°–107°E) stays over the northern Sumatran Islands (south of 6°N) from early March to mid-April, when the maximum solar heating moves from ~5°S to ~10°N. During this period, atmospheric convection is weak and shallow over the ICP, and surface solar radiation over the ICP increases rapidly and reaches a maximum around late April. This results in large surface sensible heating over the ICP land areas, which increases atmospheric instability and triggers convection over the ICP. By late April, rising motion and deep convection occur over the ICP, accompanied by descending motion over the waters to the east and west of the ICP. Strong latent heating from deep convection enhances and maintains the ascending motion and upper-level divergence, forming an anticyclonic circulation and the SAH at the 150-hPa level over the ICP.

During early–middle May, deep convection over the ICP intensifies and extends further northward and also east- and westward to over parts of the BOB and SCS. By mid-May, vigorous convection centered over the ICP produces strong updrafts and large upper-level divergence, marking the full establishment of the SAH over the ICP.

Thus, the seasonal maximum solar heating and land–sea

contrast around the ICP provide the basic conditions for deep convection to preferentially occur over the ICP, which leads to the formation of the SAH over the ICP from late April to mid-May. Simulations using RegCM4 also indicate that the diabatic heating over the ICP favors the generation and development of the upper-level anticyclonic circulation and appearance of the "two-cored" structure, which leads to the earlier establishment of the SAH.

In essence, this movement of the upper-level anticyclone from the western Pacific waters to the ICP following the maximum diabatic heating from late April to mid-May is similar to the SAH's northwestward movement to the Tibetan Plateau from late May to early June, which also follows the seasonal maximum thermal heating over Asia, as noticed previously (Qian et al., 2002; Liu et al., 2004).

Acknowledgements. The authors are grateful to Prof. Zhaoyong GUAN for his help. This work was jointly supported by the Major Program of the Natural Science Researches for Colleges and Universities in Jiangsu Province (Grant No. 14KJA170004), the Natural Science Foundation of Jiangsu Province (Grant No. BK20131432), the "333" Project of Jiangsu Province, "Qing Lan" Project of Jiangsu Province and the Priority Academic Program Development of Jiangsu Higher Education Institutions (PAPD). A. Dai was supported by the U.S. National Science Foundation (Grant No. AGS-1353740), the U.S. Department of Energy's Office of Science (Grant No. DE-SC0012602), and the U.S. National Oceanic and Atmospheric Administration (Grant No. NA15OAR4310086).

REFERENCES

Flohn, H., 1960: Recent investigation on the mechanism of the "summer monsoon" of southern and eastern Asia. *Proceedings of Symposium on Monsoon of the World*, New Delhi, Hind Union Press, 75–88.

Giorgi, F., and Coauthors, 2012: RegCM4: Model description and preliminary tests over multiple CORDEX domains. *Clim. Res.*, **52**, 7–29.

Gong, C. S., H. X. Duan, Y. H. Li, C. H. Wang, and Y. L. Ren, 2015: Simulation of temperature and precipitation in China in the last 30 years by using the RegCM4. *Journal of Arid Meteorology*, **33**, 379–385. (in Chinese)

Han, J., Z. Y. Guan, and M. G. Li, 2015: Comparisons of circulation anomalies between the daily precipitation extreme and non-extreme events in the middle and lower reaches of Yangtze River in boreal summer. *Journal of Tropical Meteorology*, **21**, 131–142.

Haque, M. A., and M. Lal, 1991: Diagnosis of satellite-derived outgoing long wave radiation in relation to rainfall in India. *Meteor. Atmos. Phys.*, **45**, 1–13.

He, J. H., H. M. Xu, L. J. Wang, and B. Zhou, 2003: Climatic features of SCS summer monsoon onset and its possible mechanism. *Acta Meteor. Sinica*, **17**, 19–34.

He, J. H., M. Wen, L. J. Wang, and H. M. Xu, 2006: Characteristics of the onset of the Asian Summer Monsoon and the importance of Asian-Australian "land bridge". *Adv. Atmos. Sci.*, **23**, 951–963, doi: 10.1007/s00376-006-0951-z.

Holtslag, A. A. M., E. I. F. De Bruijn, H. L. Pan, 1990: A high resolution air mass transformation model for short-range weather forecasting. *Mon. Wea. Rev.*, **118**, 1561–1575.

Hu, P., 2006: Research on the onset of South China Sea monsoon and the reconstructure of South Asia High. PhD dissertation, Nanjing University of Information Science & Technology, 183 pp. (in Chinese)

Kalnay, E., and Coauthors, 1996: The NCEP/NCAR 40-year reanalysis project. *Bull. Amer. Meteor. Soc.*, **77**, 437–471.

Ke, D., and Z. Y. Guan, 2014: Variations in regional mean daily precipitation extremes and related circulation anomalies over central China during boreal summer. *J. Meteor. Res.*, **28**, 524–539.

Li, C. Y., and M. Q. Mu, 2001: The dipole in the equatorial Indian Ocean and its impacts on climate. *Chinese J. Atmos. Sci.*, **25**, 433–443. (in Chinese)

Liu, B. Q., G. X. Wu, J. Y. Mao, and J. H. He, 2013: Genesis of the South Asian high and its impact on the Asian summer monsoon onset. *J. Climate*, **26**, 2976–2991.

Liu, X. F., Q. G. Zhu, and P. W. Guo, 2000: Conversion characteristics between barotropic and baroclinic circulations of the SAH in its seasonal evolution. *Adv. Atmos. Sci.*, **17**, 129–139, doi: 10.1007/s00376-000-0049-y.

Liu, Y. M., G. X. Wu, H. Liu, and P. Liu, 1999: The effect of spatially nonuniform heating on the formation and variation of subtropical high. Part III: Condensation heating and south Asia high and western Pacific subtropical high. *Acta Meteorologica Sinica*, **57**, 525–538. (in Chinese)

Liu, Y. M., G. X. Wu, and R. C. Ren, 2004: Relationship between the subtropical anticyclone and diabatic heating. *J. Climate*, **17**, 682–698.

Lu, C. H., L. Huang, J. H. He, and Y. J. Qin, 2015: Interannual variation in heat content of the western Pacific warm pool and its effect on eastern Asian climate anomalies. *Journal of Tropical Meteorology*, **21**, 246–254.

Luo, S. W., Z. A. Qian, and Q. Q. Wang, 1982: The climatic and synoptical study about the relation between the Qinghai-Xizang High pressure on the 100mb surface and the flood and drought in east China in summer. *Plateau Meteorology*, **1**, 1–10. (in Chinese)

Mason, R. B., and C. E. Anderson, 1963: The development and decay of the 100-mb summertime anticyclone over southern Asia. *Mon. Wea. Rev.*, **91**, 3–12.

Miyasaka, T., and H. Nakamura, 2005: Structure and formation mechanisms of the Northern Hemisphere summertime subtropical highs. *J. Climate*, **18**, 5046–5065.

Qian, Y. F., Q. Zhang, Y. H. Yao, and X. H. Zhang, 2002: Seasonal variation and heat preference of the South Asia High. *Adv. Atmos. Sci.*, **19**, 821–836, doi: 10.1007/s00376-002-0047-3.

Qian, Y. F., J. Jiang, Y. Zhang, Y. H. Yao, and Z. F. Xu, 2004: The earliest onset area of the tropical Asian summer monsoon and its mechanisms. *Acta Meteor. Sinica*, **62**, 129–139. (in Chinese)

Rodwell, M. J., and B. J. Hoskins, 1996: Monsoons and the dynamics of deserts. *Quart. J. Roy. Meteor. Soc.*, **122**, 1385–1404.

Rodwell, M. J., and B. J. Hoskins, 2001: Subtropical anticyclones and summer monsoons. *J. Climate*, **14**, 3192–3211.

Tan, J., H. Yang, S. Q. Yang, and P. X. Wang, 2005: Characteristics of the longitudinal oscillation of South Asia High during summer. *Journal of Nanjing Institute of Meteorology*, **28**, 452–460. (in Chinese)

Tang, W. Y., and Z. Y. Guan, 2015: ENSO-independent contemporaneous variations of anomalous circulations in the Northern

and Southern Hemispheres: The polar-tropical seesaw mode. *J. Meteor. Res.*, **29**, 917–934.

Tao, S. Y., and F. K. Zhu, 1964: The 100-mb flow patterns in southern Asia in summer and its relation to the advance and retreat of the west-Pacific subtropical anticyclone over the far east. *Acta Meteor. Sinica*, **34**, 385–396. (in Chinese)

Uppala, S. M., and Coauthors, 2005: The ERA-40 re-analysis. *Quart. J. Roy. Meteor. Soc.*, **131**, 2961–3012.

Wu, G. X., and Y. S. Zhang, 1998: Tibetan Plateau forcing and the timing of the monsoon onset over South Asia and the South China Sea. *Mon. Wea. Rev.*, **126**, 913–927.

Wu, G. X., B. He, Y. M. Liu, Q. Bao and R. C. Ren, 2015: Location and variation of the summertime upper-troposphere temperature maximum over South Asia. *Climate Dyn.*, **45**, 2757–2774.

Yanai, M., S. Esbensen, and J. H. Chu, 1973: Determination of bulk properties of tropical cloud clusters from large-scale heat and moisture budgets. *J. Atmos. Sci.*, **30**, 611–627.

Yang, H., and C. Y. Li, 2005: Effect of the tropical Pacific-Indian Ocean temperature anomaly mode on the South Asia High. *Chinese J. Atmos. Sci.*, **29**, 99–110. (in Chinese)

Zeng, X. B., M. Zhao, and R. E. Dickinson, 1998: Intercomparison of bulk aerodynamic algorithms for the computation of sea surface fluxes using TOGA COARE and TAO data. *J. Climate*, **11**, 2628–2644.

Zhang, Q. Y., Z. H. Jin, and J. B. Peng, 2006: The relationships between convection over the Tibetan Plateau and circulation over East Asia. *Chinese J. Atmos. Sci.*, **30**, 802–812 (in Chinese).

Zhang, S. B., S. H. Lv, Y. Bao, and D. Ma, 2015: Sensitivity of precipitation over China to different cumulus parameterization schemes in RegCM4. *J. Meteor. Res.*, **29**, 119–131.

Zhang, Y. C., and Y. F. Qian, 2002: Mechanism of thermal features over the Indo-China Peninsula and possible effects on the onset of the South China Sea monsoon, *Adv. Atmos. Sci.*, **19**, 885–900, doi: 10.1007/s00376-002-0053-5.

Zhu, F. K., and Coauthors, 1980: The South Asian Highs. Science Press, Beijing, 95 pp. (in Chinese)

Zhu, Q. G., and J. H. He, 1985: On features of the upper circulation in the establishment of Asian monsoon in 1979 and its medium-range oscillation. *Journal of Tropical Meteorology*, **1**, 9–18. (in Chinese)

Zou, J., and Z. H. Xie, 2012: The effects of the land-surface process parameterization of the RegCM4 on climate simulation in East Asia. *Acta Meteor. Sinica*, **70**, 1312–1326. (in Chinese)